A Journal of the Gesellschaft Deutscher Chemiker

Angewandte International Edition

GDCh

Chemie

www.angewandte.org

Accepted Article

Title: Self-reporting inhibitors: single crystallization process to get two optically pure enantiomers

Authors: Xinhua Wan, Xichong Ye, Jiaxi Cui, Bowen Li, Na Li, and Jie Zhang

To be cited as: *Angew. Chem. Int. Ed.* 10.1002/anie.201803480
Angew. Chem. 10.1002/ange.201803480

Link to VoR: http://dx.doi.org/10.1002/anie.201803480
http://dx.doi.org/10.1002/ange.201803480

WILEY-VCH

10.1002/anie.201803480

WILEY-VCH

Self-reporting inhibitors: single crystallization process to get two optically pure enantiomers

Xichong Ye,[a]¶ Jiaxi Cui,[b]¶ Bowen Li,[a] Na Li,[a] Jie Zhang,[a] and Xinhua Wan*[a]

Abstract: Collection of two optically pure enantiomers in a single crystallization process can significantly increase the chiral separation efficiency but it's hard to realize nowadays. Herein we describe, for the first time, a self-reporting strategy for visualizing the crystallization process by a kind of dyed self-assembled inhibitors made from the copolymers with tri(ethylene glycol)-grafting polymethylsiloxane as main chains and poly(N^6-methacryloyl-*L*-lysine) as side chains. When applied with seeds together for the fractional crystallization of conglomerates, the inhibitors can label the formation of the secondary crystals and guide us to completely separate the crystallization process of two enantiomers with colorless crystals as the first product and red crystals as the secondary product. This method leads to high optical purity of *D*/*L*-Asn·H_2O (99.9 ee% for *D*-crystals and 99.5 ee% for *L*-crystals) in a single crystallization process. Moreover, it requires low feeding amount of additives and shows excellent recyclability. We foresee its great potential in developing novel chiral separation methods that can be used in different scales.

Crystallization is a powerful separation technique to produce pure chemicals in large scale.[1] Essential to this ancient method, target product has a different solubility from impurities to precipitate as a pure compound.[2] For getting high yield and purity of a product, the (re)crystallization conditions should be optimized to allow maximally product to precipitate before impurities crystallize. It is a highly efficient method to purify a product containing minority impurities with distinguishing physical properties and has constituted a protocol used in both lab and plant. However, its applicability is significantly hindered in the separation of the racemic mixture in which two enantiomers have identical physical properties. To get optically pure enantiomers—essential compounds for modern pharmacy and agrochemistry[3]—from the conglomerates,[4] chiral additives are utilized to tune the crystallization kinetics of the enantiomers.[5] The approaches currently available include adding a chiral seed to reduce the nucleation barrier of one enantiomer for preferential crystallization (PC)[6] and applying "tailor-made" additives for selectively inhibiting the growth of one enantiomer to allow another to crystallize.[7] These fractional crystallization methods are the main strategy to get enantiopure compounds in industry but their separation efficiencies are low, typically in a region of 10~20%, because of kinetic resolution nature (Figure 1a).[8] It is extremely challenging to collect both optically pure enantiomers in a single crystallization process due to the difficulty in noting the critical point of another enantiomer to precipitate and then being able to make a complete separation of the crystallization of two enantiomers.[9] Great progress has been made in the rapid determination of enantiomeric excess by optical approaches.[10] However, more efficient fractional crystallization methods for chiral resolution of conglomerates, especially of non-racemizing conglomerate crystals, remains to be developed.[11] We describe herein a class of self-reporting inhibitors that permit direct readout of the crystallization of another enantiomer and then guide us to obtain a complete separation of the crystallization processes of two enantiomers.

Our self-reporting inhibitors are made from the copolymers with tri(ethylene glycol)-grafting polymethylsiloxane (PMS-*g*-TEG) as the main chain and poly(N^6-methacryloyl-*L*-lysine) (PMAL) as the side chains (*L*-P-P-n, n represents the number-averaged polymerization degree of PMAL). Their counterparts containing *D*-lysine were also prepared (*D*-P-P-n). The synthesis and characterization of these polymers are shown in Supporting information (Scheme S1 and Figures S1-S8). Under our reaction conditions, the molar ratio of PMAL and tri(ethylene glycol)alkyl in the grafted product was 1:39, which implied a T-shape structure for the *L*-P-P-n (Figure 1b). In the cycloaddition reaction, disodium sulphonated bathophenanthroline (DSB) was used as the ligand for hindering the binding of Cu(I) to the PMAL side chains.[12] This ligand remained in *L*-P-P-n after the reaction and purification process, which made the product colorful.

In *L*-P-P-n, the PMAL side chains are complete hydrophilic while the PMS-*g*-TEG main chain is thermo-responsive with lower critical solution temperature (LCST)[13] and becomes hydrophobic in supersaturated amino acid (a.a.) aqueous solution at room temperature (rt, 25 °C), due to the repulsion between TEG and hydrophilic a.a..[14] As a result of this dynamic amphiphilic structure, *L*-P-P-n self-assembles into micelles with soft PMS-*g*-TEG as core and chiral PMAL chains as arms in a.a. aqueous solution at rt (Figure 1b). The micelles would disassemble when solution temperature is low because the PMS-*g*-TEG main chain becomes hydrophilic even in a.a. aqueous solutions (Table S3 and Figure S11).

Figure 1c illustrates our strategy for selective fractional crystallization of conglomerates with *L*-P-P-n-based micelles as dyed inhibitors. Racemic amino acids were selected as model substrates because of their wide applications. Both *D*-seeds and *L*-P-P-n were added in our method to get maximal separation of the crystallization process of two enantiomers. The seed was expected to accelerate the crystallization of one enantiomer (i.e. *D*-a.a), resulting in a typical colorless crystal, while the polymeric assemblies would delay the formation of the nuclei of the other enantiomer (i.e. *L*-a.a) during the crystallization of *D*-a.a.,[15] and

[a] X. C. Ye, B. W. Li, N. Li, Prof. J. Zhang, Prof. X. H. Wan
Beijing National Laboratory for Molecular Sciences, Key Laboratory of Polymer Chemistry and Physics of Ministry of Education, College of Chemistry and Molecular Engineering, Peking University, Beijing 100871, China.
E-mail: xhwan@pku.edu.cn
[b] Dr. J. X. Cui
INM - Leibniz Institute for New Materials, Campus D22, 66123, Saarbrucken, Germany.

Supporting information for this article is given via a link at the end of the document.

¶ Equal contribution

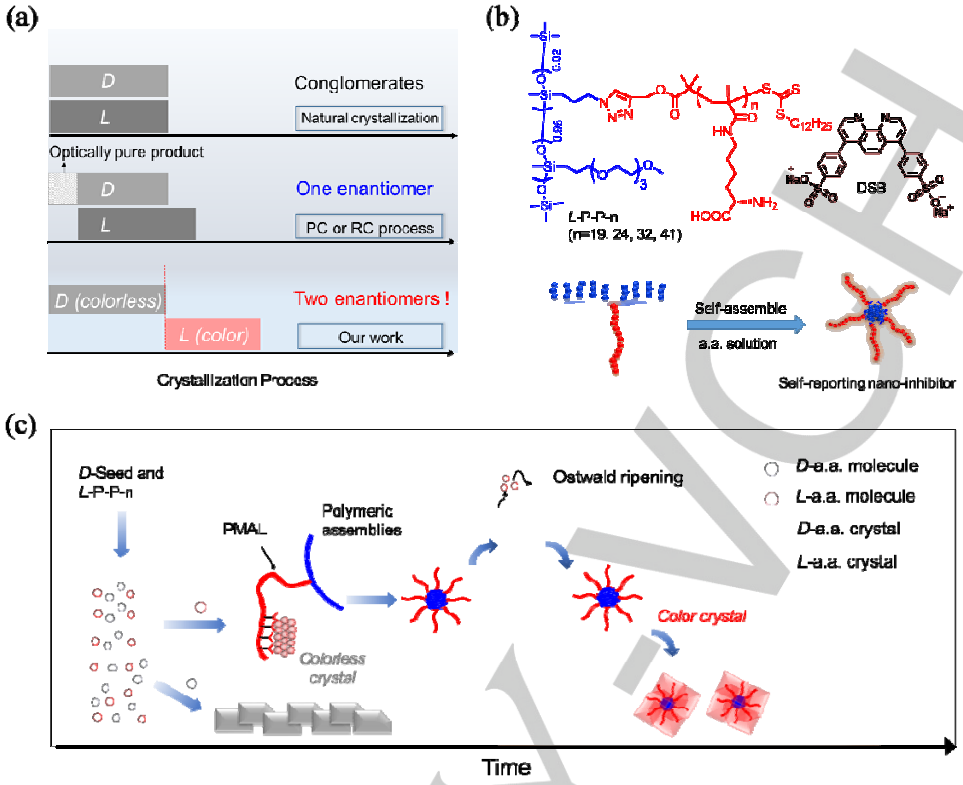

Figure 1. Collection of two enantiomers in a single crystallization process. a) The schematic concept of our strategy. b) The molecular design of *L*-P-P-n and their self-assembly in amino acids solutions. c) Proposed crystallization process in presence of both seed and inhibitors and the self-reporting mechanim.

Table 1. The resolution results of *rac*-Asn•H_2O and *rac*-Thr using *L*-P-P-24 as additive

Crystals	Asn•H_2O[a]			Thr[b]		
	ee %[c]	ee %[d]	Yield/ %	ee %[e]	ee %[f]	Yield/ %[g]
Colorless crystals (*D*)	99.9	99.9	16.9	99.9	99.9	15.6
Red crystals (*L*)	98.4	99.5	13.8	98.6	98.4	18.5

[a] Weight% of *L*-P-P-24, 4.5%; Crystallization temperature, 25 °C; Crystallization time, 48 h. [b] Weight% of *L*-P-P-24, 4.5%; Crystallization temperature, 25 °C; Crystallization time, 60 h. [c] and [e] Measured by polarimeter. [d] and [f] Measured by chiral HPLC. [g] The yield is defined as the weight ratio of the precipitated crystals/total racemic mixture.

promote the crystallization of *L*-a.a. after the crystallization of *D*-a.a.. The *L*-a.a. crystal finally formed, wrapping the dyed polymer to make the crystal colorful. In the other words, the appearance of color crystal would indicate the critical time point for *L*-a.a crystal to form. Although other strategies, like using colored seeds, can also visualize the chiral sense of $NaClO_3$ crystals,[16] such self-reporting characteristic has never been reported, which allowed us to optimize our conditions easily for completely isolating the crystallization processes of two enantiomers.

rac-Asparagine monohydrate (*rac*-Asn•H_2O) was used to demonstrate the self-reporting selective crystallization process induced by *L*-P-P-n. The crystallization condition reported in the previous publication was chosen.[7e] As *L*-P-P-24 was added into the oversaturated solution, only colorless *D*-Asn•H_2O crystals precipitated in the first 14 hours (Figure 2a). Afterward, red crystals began to form, which were confirmed to be pure *L*-Asn•H_2O. Interestingly, the colorless *D*-Asn•H_2O crystals were prismatic and small while the red *L*-Asn•H_2O ones were pyramidal and significantly larger. More importantly, the crystallization processes of two enantiomers were completely separated under optimized conditions (4.5 wt% *L*-P-P-24 in *rac*-Asn•H_2O solution at a concentration of 111 mg•mL^{-1}): the red crystals did not form until the colorless crystals completely precipitated (Figure 2b). As a result of the well-separation, this single crystallization process led to both enantiomers with extremely high optical purity (enantiomeric excess (ee)%: 99.9% for *D*-Asn•H_2O and 99.5% for *L*-Asn•H_2O) and a high total yield of 30.7%. Similar results were also obtained when our method was applied to separate *rac*-Threonine (Table 1 and Figure S14). When *D*-P-P-24 was used, the order of the formation of *D*- and *L*-crystals was reversed (Figure S15 and Table S4), which confirmed that the inhibiting effect depended on the configuration of lysine groups.

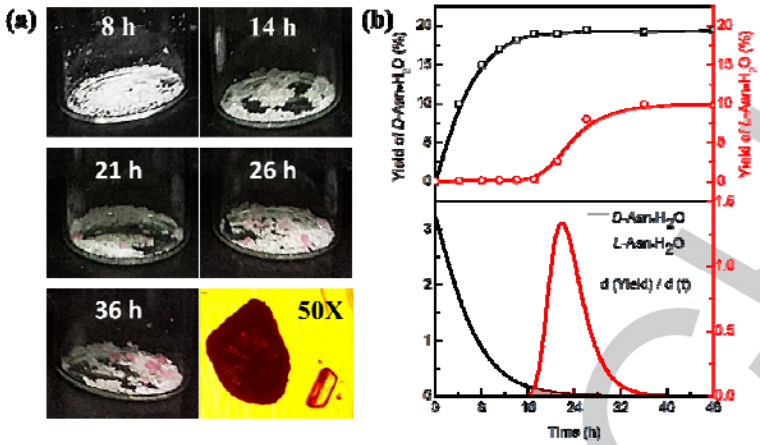

Figure 2. The stepwise crystallization process of *D*/*L*-Asn with *L*-P-P-24 as the inhibitor. a) The image of the Asn•H_2O crystals precipitated from the solution at different times and the last image is the microscope photo of the final crystals (the larger one is red crystal, the smaller one is colorless crystal). b) Plot of crystal compositions and changes over time.

It was considered that the *L*-P-P-n assemblies were entrapped in the *L*-crystals to make *L*-Asn•H_2O crystal colorful (Figure 1c). Both Asn•H_2O crystals obtained were re-dissolved and studied by ^{1}H NMR and UV spectroscopy. The presence of *L*-P-P-n in the red crystal was confirmed by ^{1}H NMR spectrum which showed the characteristic peaks of *L*-P-P-n and DSB (Figure 3a). The solution made from colorless crystal illustrated a typical spectrum of Asn•H_2O without absorption in visible-light region while the solution made from red crystal displayed obvious absorption in the region of 400-600 nm (Figure 3c). The image was identical to that of *L*-P-P-n themselves (Figure 3b), further supporting the direct connection between the color of the red crystal and the dyed polymers. Since both PMS-*g*-TEG main chain and PMAL side chains in *L*-P-P-n are colorless, we assigned the color to the residual DSB bonded on *L*-P-P-n (Figure S7). Although DSB solution shows almost no absorption in the visible region (Figure 3b and Figure S18), the solid state of it shows absorption in the region of 400-600 nm where intramolecular rotations of the aromatic moieties are restricted (Figure S17a). Because DSB remained in the *L*-P-P-n even after serious separation protocol, we expected strong noncovalent interactions between DSB and *L*-P-P-n. Such interactions might restrict the mobility of DSB molecules and made them absorptive in the visible region.[17] To prove this, a model complex made from PMAL and DSB was prepared and characterized. As expected, the complex showed identical absorption spectrum as *L*-P-P-n solutions (Figure 3b). The interactions between DSB and *L*-P-P-n were further confirmed by the circular dichroism (CD) spectra of the model complex in which induced CD signals of DSB were found (Figure S17b).

Fluorescence spectroscopy was also applied to study the presence of *L*-P-P-n in *L*-crystals. The solution made from the red crystal showed significant higher emission than that of the colorless crystal, and the image was identical with that of *L*-P-P-n themselves (Figure S19). Besides, the 3D fluorescent image of the red crystals obtained released that the *L*-P-P-n concentrated on both the core and the surface of the crystal (Figure 3e). The presence of *L*-P-P-n in the core suggested that the polymeric assemblies were entrapped in the crystal at the very beginning of the crystallization process.

We proposed that the formation of red crystals involved an enriching process of *L*-a.a. clusters on the polymeric assemblies and an Ostwald ripening process.[18] The *L*-a.a. clusters, that were smaller than the critical nucleus size, were entrapped by the PMAL arms. Such enriching process was supported by light scattering results in which the size of the assemblies continually increases before forming macroscopic crystals (Figure S20). An Ostwald ripening process might occur in the cluster-enriched polymeric assemblies (Figure S21), which led to a high local *L*-a.a. concentration to trigger nucleation.[19] After the dyed core formed, small a.a. molecules, rather than *L*-P-P-n, selectively deposit on the growing crystal planes, leading to the dye-free middle region. Since the red crystal showed the same X-ray diffraction to the colorless one (same to as-grown Asn•H_2O, Figure S22).[20] We did not expect any difference in this crystal growth process from colorless one. The *L*-P-P-n polymers finally attached to the surface of grown crystals when no excess a.a. molecules were available in the solution.

The fractional crystallizations of Asn•H_2O were carried out at the other two concentrations. At a concentration of 91 mg•mL^{-1}, only colorless crystals were obtained, while poor separation effect was observed at a concentration of 154 mg•mL^{-1} (Table S5 and Figure S24). This phenomenon was rationalized by the solubility and metastable zone curves of Asn•H_2O.[21] At a lower concentration, the supersaturation of Asn•H_2O was under the boundary of metastable zone and PC dominanted in a limited crystallization time, leading to colorless *D*-crystals. The disassembly of micelles at this concentration is another important factor (Figure. S23). At the concentration of 154 mg•mL^{-1}, which is far above the boundary of metastable zone, *L*-Asn•H_2O tended to nucleate spontaneously and precipitate together with *D*-Asn•H_2O crystals. As for the concentration of 111 mg•mL^{-1}, which is a little above the critical boundary of metastable zone, *D*-Asn•H_2O crystallized first, while the nucleation and crystal growth of *L*-Asn•H_2O was inhibited. After the crystallization of *L*-Asn•H_2O was over, the clusters of *L*-Asn•H_2O captured by *L*-PMAL side chains became beyond the critical size owing to Ostwald ripening, causing spontaneous crystallization of *L*-Asn•H_2O.

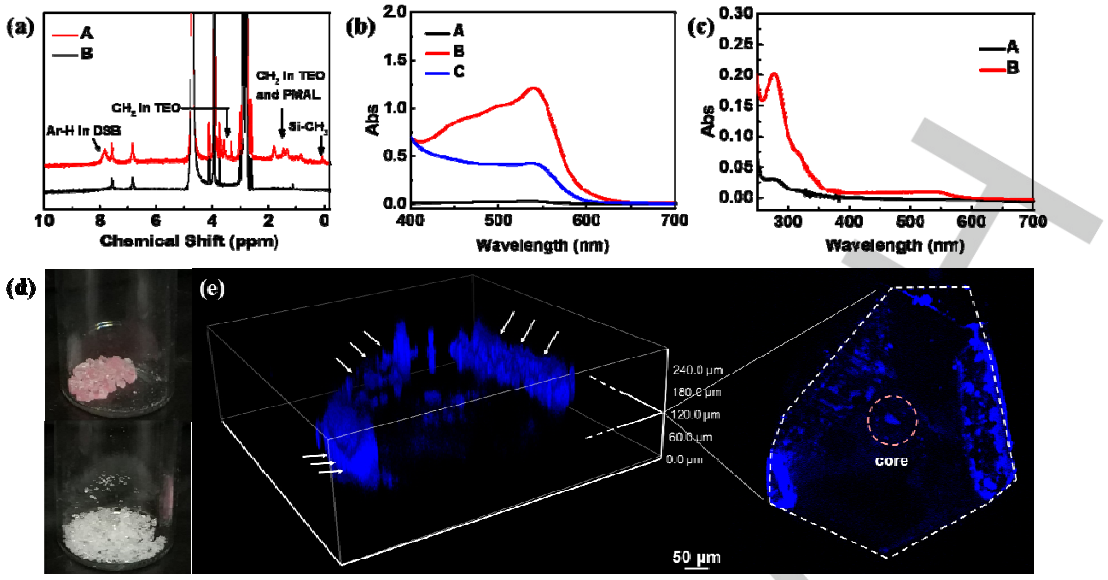

Figure 3. Self-reporting mechanism. a) ^{1}H NMR spectra of the solution of crystals in D_2O (A: solution of red crystals; B: solution of colorless crystals). b) UV-vis absorption spectra (A: solution of DSB (0.5 mg•mL^{-1}); B: solution of DSB (0.5 mg•mL^{-1}) and PMAL (n=24) (10 mg•mL^{-1}), C: solution of *L*-P-P-24 (20 mg•mL^{-1})). c) UV-vis absorption spectra of the aqueous solution of crystals with a concentration of 20 mg•mL^{-1} (A: solution of colorless crystals; B: solution of red crystals). d) The red and colorless crystals obtained by using *L*-P-P-24 as an additive. e) The 3D confocal fluorescence image of the red crystals (3D image on the left and horizontal cross-section on right). Arrows highlight the crystal surfaces.

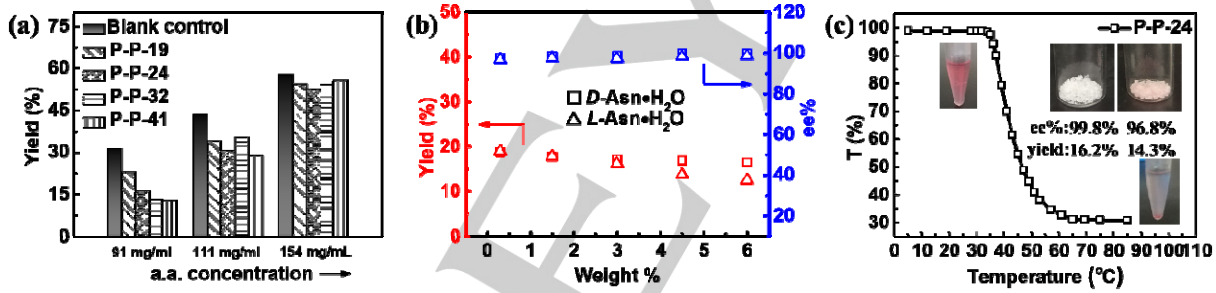

Figure 4. The other advantages of using *L*-P-P-n for resolution of a.a.. a) The comparison among limit crystal yields at different a.a. concentrations. b) Plot of feeding amount of *L*-P-P-24 and crystallization yield/ee% of products. Total crystallization time: 48 h; concentration of *rac*-Asn•H_2O: 111 mg•mL^{-1}. c). The transmittance of *L*-P-P-24 solution (5 mg•mL^{-1}) at different temperature and the crystallization results by using the recycled *L*-P-P-24.

The length of *L*-PMAL side chains also significantly affect the resolution results. Among the four polymers employed, only *L*-P-P-24 allowed *D*-Asn•H_2O crystals to completely precipitate before *L*-Asn•H_2O crystals appeared (Table S6). This may be rationalized by the critical interfacial hydrophobicity caused by the side chains. *L*-P-P-n used acted as the inhibitors through the formation of core-shell aggregates, the morphologies of which were determined by the relative ratio of hydrophobic and hydrophilic parts. As indicated by the light scattering results (Table S3), vesicles were formed by *L*-P-P-19, spherical micelles by *L*-P-P-24 and *L*-P-P-32, and rod-like micelles by *L*-P-P-41. The chiral resolution by *L*-P-P-19 was poor since only outer parts of vesicles played a role in inhibiting the growth of *L*-crystals. For the other three polymers with long hydrophilic side chains, the dependence of inhibiting effect on the side chain length may be related to the "effective local concentration".[8d]

In addition to the self-reporting mechanism and getting two enantiomers in a single crystallization process, we also claim other advantages of our strategy, including high crystallization yield,[7e, 21a] low feeding amount, and recyclability. Figure 4a illustrates the maximal crystallization yields of test groups under different a.a. supersaturation with blank a.a. solution as the controls. The maximal crystallization yields of the test groups were close to the control ones. The total crystallization yields were significantly higher than the typical crystallization yield of 20% obtained in traditional inhibitor-based crystallization.[8] On the other hand, the feeding amount of the inhibitor could lower to 0.3 wt% without compromising the selection effect (Figure 4b and Table S7-S9).[22] Moreover, *L*-P-P-n was thermo-responsive in aqueous solution and underwent macroscopic phase separation in a.a. solution at high temperatures (e.g. 42 °C in Figure 4c).[23] *L*-P-P-n could be easily recollected by elevating the temperature. The same method could also be used to collect the polymers wrapped in the red crystals. After simple water-washing, the polymer collected can be reused directly without reducing any performance.

Our methodology has been extended to an additional system. By replacing the lysine units in *L*-P-P-n with *L*-phenylalanine,

another copolymer, *L*-P-PMP (Scheme S1 and Figures S9 and S10), was obtained. It can mediate the crystallization of racemic *p*-hydroxyphenylglycine *p*-toluenesulfonate (*rac*-*p*Hpg*p*Ts) and lead to similar crystallization results (Figure S16).

In summary, we have reported a novel strategy for selective fractional crystallization of conglomerates in which the precipitation of the second enantiomer can be directly read out from the crystal color by using a kind of self-reporting inhibitors. Completely isolation of the crystallization processes of two enantiomers can be realized. The performances are significantly better than the state-of-the-art methods, although this strategy only works in the case of conglomerates at this stage and the productivity should be further improved in practical application.[21b] It might open a window for developing more efficient fractional crystallization methods and be potential in the chiral separation in different scales.

Acknowledgements

We gratefully acknowledge the financial supports from the National Natural Science Foundation of China (No. 21674002). We acknowledge the support from BMBF under the project of the Leibniz Research Cluster with an award number 031A360D. We thank Dr. Yan Guan for her help with the confocal microscopy measurements.

Keywords: self-reporting • inhibitor • chiral resolution • self-assembly • polymers

[1] D. Erdemir, A. Y. Lee, A. S. Myerson, *Acc. Chem. Res.* **2009**, *42*, 621-629.

[2] R. Kumar, D. Vikramachakravarthi, P. Pal, *Chem. Eng. Process* **2014**, *81*, 59-71.

[3] S. Itsuno, *Polymeric Chiral Catalyst Design and Chiral Polymer Synthesis*, Wiley, Hoboken, New Jersey, **2011**, pp. 17-18.

[4] a) J. Jacques, A. Collet, S. H. Wilen, *Enantiomers, Racemates, and Resolutions*, Wiley-VCH, Weinheim, **1981,** pp. 139; b) A. Collet, M. J. Brienne, J. Jacques, *Chem. Rev.* **1980**, *80*, 215-230; c) A. Otero-de-la-Roza, J. E. Hein, E. R. Johnson, *Cryst. Growth Des.* **2016**, *16*, 6055-6059.

[5] a) R. Q. Song, H. Cöfen, *CrystEngComm* **2011**, *13*, 1249-1276; b) E. Elfassy, Y. Basel, Y. Mastai, *CrystEngComm* **2016**, *18*, 8769–8775.

[6] a) D. D. Medina, J. Goldshtein, S. Margel, Y. Mastai, *Adv. Funct. Mater.* **2007**, *17*, 944-950; b) B. Chen, J. P. Deng, W. T. Yang, *Adv. Funct. Mater.* **2011**, *21*, 2345-2350; c) L. Yang, Y. Tang, N. Liu, C. H. Liu, Y. S. Ding, Z. Q. Wu, *Macromolecules* **2016**, *49*, 7692-7702; d) L. Y. Pfund, C. P. Price J. J. Frick, A. J. Matzger, *J. Am. Chem. Soc.* **2015**, *137*, 871-875; e) Y. Huang, Y. Jiang, X. R. Yang, Y. Ren, D. Zhan, H. Cölfen, Z. Q. Hou, *Cryst. Growth Des.* **2016**, *16*, 1428-1434;

[7] a) L. Addadi, Z. Berkovitch-Yellin, N. Domb, E. Shavit-Gati, M. Lahav, L. Leiserowitz, *Nature* **1982**, *296*, 21-26; b) L. Addadi, E. Shavit-Gati, M. Lahav, *J. Am. Chem. Soc.* **1981**, *103*, 1251-1252; c) L. Addadi, J. Van Mil, M. Lahav, *J. Am. Chem. Soc.* **1981**, *103*, 1249-1251; d) L. Addadi, S. Weinstein, E. Shavit-Gati, I. Weissbuch, M. Lahav, *J. Am. Chem. Soc.* **1982**, *104*, 4610-4617. e) D. Zbaida, I. Weissbuch, E. Shavit-Gati, L. Addadi, L. Leiserowitz, *React. Polym.* **1987**, *6*, 241-253; f) Y. Mastai, M. Sedlák, H. Cölfen, M. Antonietti, *Chem.-Eur. J.* **2002**, *8*, 2429-2437; g) S. Wohlrab, N. Pinna, M. Antonietti, H. Cölfen, *Chem.-Eur. J.* **2005**, *11*, 2903-2913; h) J. Anwar, P. K. Boateng, R. Tamaki, S. Odedra, *Angew. Chem. Int. Ed.* **2009**, *121*, 1624-1628. i) J. D. Rimer, Z. An, Z. Zhu, M. H. Lee, D. S. Goldfarb, J. A. Wesson, M. D. Ward, *Science* **2010**, *330*, 337-341; j) T. P. T. Nguyen, P. S. M. Cheung, L. Werber, J. Gagnon, R. Sivakumar, C. Lennox, A. Sossin, Y. Mastai, L. A. Cuccia, *Chem. Commun.* **2016**, *52*, 12626-12629; (k) P. Kongsamai, A. Maneedaeng, C. Flood, J. H. ter Horst, A. E. Flood, *Eur Phys J-Spec Top*, **2017**, *226*, 823–835.

[8] a) T. Menahem, Y. Mastai, *J. Polym. Sci., Part A: Polym. Chem.* **2006**, *44*, 3009-3017; b) K. Würges, K. Petruševska-Seebach, M. P. Elsner, S. Lütz, *Biotechnol. Bioeng*. **2009**, *104*, 1235-1239; c) H. Lorenz, A. Seidel-Morgenstern, *Angew. Chem. Int. Ed.* **2014**, *53*, 1218-1250; d) N. Li, H. Wang, J. Zhang, X. H. Wan, *Polym. Chem.* **2014**, *5*, 1702-1710.

[9] a) T. Ushio, R. Tamura, H. Takahashi, N. Azuma, K. Yamamoto, *Angew. Chem. Int. Ed.* **1996**, *35*, 2372-2374; b) R. Tamura, D. Fujimoto, Z. Lepp, K. Misaki, H. Miura, H. Takahashi, T. Ushio, T. Nakai, K. Hirotsu, *J. Am. Chem. Soc.* **2002**, *124*, 13139-13153; c) L. Zhang, L. Qin, X. F. Wang, H. Cao, M. H. Liu, *Adv. Mater.* **2014**, *26*, 6959-6964; d) T. Tu, W. Fang, Z. Sun, *Adv. Mater.* **2013**, *25*, 5304-5313.

[10] a) D. Leung, S. O. Kang, E. V. Anslyn, *Chem. Soc. Rev.*, **2012**, *41*, 448-479; b) X. Mei, C. Wolf, *Chem. Commun*. **2004**, 2078-2079. c) L. Zhu, Z. L. Zhong, E. V. Anslyn, *J. Am. Chem. Soc*. **2005**, *127*, 4260-4269. d) P. Paik, A. Gedanken, Y, Mastai, *Acs Appl. Mater. Interfaces*, **2009**, *8*, 1834-1842.

[11] J. E. Hein, B. H. Cao, C. Viedma, R. M. Kellogg, D. G. Blackmond, *J. Am. Chem. Soc*. **2012**, *134*, 12629-12636.

[12] M. Kar, P. S. Vijayakumar, B. L. Prasad, S. S. Gupta, *Langmuir* **2010**, *26*, 5772-5781.

[13] Y. J. Zheng, X. Liu, J. J. Xu, H. X. Zhao, X. H. Xiong, X. Hou, J. X. Cui, *Acs Appl. Mater. Interfaces* **2017**, *9*, 35483-35491.

[14] a) K. Sasahara, H. Uedaira, *Colloid Polym Sci* **1993**, *271*, 1035-1040; b) E. Nosaibah, S. Rahmat, *J. Chem. Thermodyn* **2015**, *90*, 129-139; c) Y. Nozaki, C. Tanford, *J. Biol. Chem.* **1965**, *240*, 3568-3573.

[15] N. Kubota, J. W. Mullin, *J. Cryst. Growth* **1995**, *152*, 203-208.

[16] C. Viedma, J. M. McBride, B. Kahr, P. Cintas, *Angew. Chem. Int. Ed.* **2013**, *52*, 10545-10548.

[17] V. Percec, A. E. Dulcey, V. S. K. Balagurusamy, Y. Miura, J. Smidrkal, M. Peterca, S. Nummelin, U. Edlund, S. D. Hudson, P. A. Heiney, H. Duan, S. N. Magonov, S. A. Vinogradov, *Nature* **2004**, *430*, 764-768.

[18] a) W. Ostwald, *Zeitschrift für physikalische Chemie* **1897**, *22*, 289-330; b) Z. Huang, M. Su, Q. Yang, Z. Li, S. Chen, Y. Li, X. Zhou, F. Li, Y. Song, *Nat. Commun.* **2017**, *8*, 14110.

[19] D. Kashchiev, G. Van Rosmalen, *Cryst. Res. Technol.* **2003**, *38*, 555-574.

[20] M. Shakir, S. Kushawaha, K. Maurya, S. Kumar, M. Wahab, G. Bhagavannarayana, *J. Appl. Crystallogr.* **2010**, *43*, 491-497.

[21] (a) K. Petruševska-Seebach, A. Seidel-Morgenstern, M. P. Elsner, *Cryst. Growth Des*. **2011**, *11*, 2149–2163; (b) D. Binev, A. Seidel-Morgenstern, H. Lorenz, *Cryst. Growth Des.* **2016**, *16*, 1409-1419

[22] S. Kojo, H. Uchino, M. Yoshimura, K. Tanaka, *Chem. Commun.* **2004**, 2146-2147.

[23] X. C. Ye, J. Zhang, J. X. Cui, X. H. Wan, *Chem. Commun.* **2018**, *54*, 2785-2787.

10.1002/anie.201803480

WILEY-VCH

Entry for the Table of Contents (Please choose one layout)

COMMUNICATION

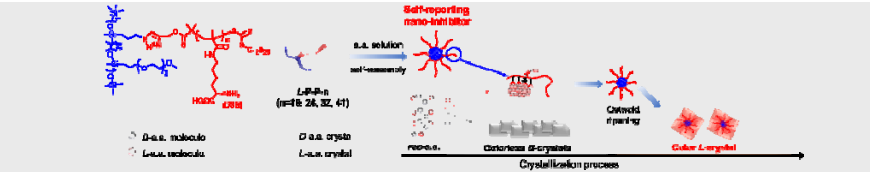

*Xichong Ye,[¶] Jiaxi Cui,[¶] Bowen Li, Na Li, Jie Zhang, Jiaxi Cui, Xinhua Wan**

Page No. – Page No.

Self-reporting inhibitors: single crystallization process to get two optically pure enantiomers

Text for Table of Contents

Small amount of recyclable, dyed self-assembled inhibitors made from the dynamic amphiphilic copolymers, consisting of tri(ethylene glycol)-grafting polymethylsiloxane main chains and poly(N^6-methacryloyl-*L*-lysine) side chains, completely separate the crystallization process of two enantiomeric amino acids with colorless crystals as the first product (99.9 ee%) and red crystals as the second one (99.5 ee%) in a single crystallization process.